



A Bayesian conformity and risk assessment adapted to a form error model

ARTICLE INFO

Keywords

Bayesian inference
Conformance assessment
Form error
Specific risks
Uniform distribution
Measurement uncertainty

ABSTRACT

Form error is the departure of a manufactured part from its design or ideal shape, and is a key characteristic to be assessed in quality engineering in manufacturing. In practice, form errors are usually estimated from coordinate measurements involving only a finite number of measured points and the form error for the complete workpiece surface has to be inferred on the basis of these measurements. This paper is about determining whether a product meets its specifications based on its form error using a probabilistic model. Based on form error data and a product specification, the relationship between conformance testing and making decisions is established. In this paper, we define a form error model using a uniform distribution with unknown bounds, and then utilize a Bayesian approach to assign a distribution to the form error parameter and use this distribution in a conformity and risk assessment methodology to quantify the risk of incorrect decisions. The risk assessment is carried out using derived expressions of specific risks associated with product conformity. A slightly more extensive posterior model, taking into consideration the probable random effects of form errors, is discussed for the reader's interest. Numerical experiments illustrate the effectiveness of this approach by providing a decision framework to control the risks associated with making a wrong decision.

1. Introduction

Form error is the departure of a manufactured part from its design or ideal shape and is a key characteristic to be assessed in quality engineering in manufacturing. In practice, form errors are usually estimated from coordinate measurements involving only a finite number of measured points and the form error for the complete workpiece surface must be inferred based on these measurements. This paper is concerned with determining whether a product meets its specifications based on its measured form error. Form is one of three major elements constituting surface measurement and topography; the other two being: roughness and waviness of the surface profile. Form errors are important for product functionalities, such as shaft vibration. A form measurement is performed to assess the general shape of an item under study, which may refer to its flatness, straightness, circularity, parallelism, roundness, or cylindricity. The assessment of form error involves two computational steps: calculating some measure of the distance $f_i(x_i, \mathbf{a})$ of a point $x_i = (x_i, y_i, z_i)$ to the ideal geometry parametrized by parameters $\mathbf{a} = (a_1, \dots, a_m)^T$ and then adjusting \mathbf{a} so that some aggregate measure $D(\mathbf{a})$ of distance is minimised; see e.g., Refs. [1–3].

For example, a circle can be parametrized by circle centre coordinated (x_0, y_0) and radius r_0 . The form error $f_i(x_i, \mathbf{a})$, for $i = 1, 2, \dots, m$, from a point $x_i = (x_i, y_i)$ to a circle specified by $\mathbf{a} = (x_0, y_0, r_0)$ is given by:

$$f_i(x_i, \mathbf{a}) \equiv f_i = [(x_i - x_0)^2 + (y_i - y_0)^2]^{1/2} - r_0.$$

A vector of these estimates is given by $\mathbf{f} = (f_1, \dots, f_m)^T$. An estimate F for the maximum form error is given by $F = \max f_i - \min f_i$. For form error expressions for other standard geometric shapes, see Ref. [1].

All measurements are subject to uncertainty and the measurement result is complete only if it is supplemented by a declaration of the associated uncertainty, such as the standard deviation. A popular way to obtain form error data is by means a coordinate measuring machine (CMM) which are used extensively for this task. If a product is measured with a CMM at a specified number of points, we want to know whether the product meets the tolerances based on the measured results. The introduction of CMMs in manufacturing has made quality assurance more effective, precise, and adaptable.

Two aggregate measures of distance $D(\mathbf{a})$ are commonly used. The first is least squares (LS) method $D_{LS}(\mathbf{a}) = \sum_i f_i^2(\mathbf{a})$, and the second is the

Chebyshev measure (also known as the minimum zone (MZ)) $D_{MZ}(\mathbf{a}) = \max |f_i(\mathbf{a})|$. A visual example for estimating the form error on a circular item with centre (x_0, y_0) and radius r_0 from a CMM is provided in Fig. 1.

Since the form error of a part is usually defined as the maximum departure (distance) from ideal geometry, the MZ criterion is often preferred as it represents the assessing the form error directly based on a discrete representation of the workpiece via the measured coordinated x_i . These aggregate measures will depend nonlinearly on the parameters \mathbf{a} so that iterative optimisation techniques are required to minimise them. In general, algorithms for nonlinear least squares optimisation are much more straight forward to implement than those for nonlinear Chebyshev optimisation. For problems that are linear in the parameters \mathbf{a} , there are effective algorithms for the Chebyshev and related optimisation problems; see for example, [4–6]. The nonlinear associated problem can sometimes be addressed through solving a sequence of linearised problems [7].

A statistical analysis methodology can be utilized to evaluate the conformance of the measurand with a given tolerance limit, and a

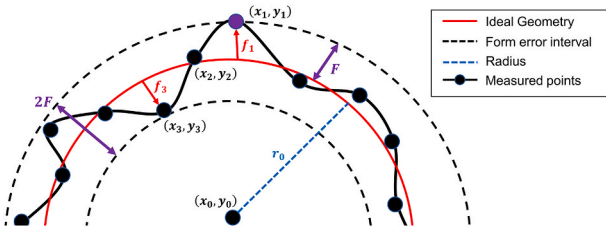


Fig. 1. Form error fitting of a circular item with centre (x_0, y_0) , radius r_0 and several measured points consisting of m discrete points for estimates f . Form generated by least squares method.

probability density function (PDF) characterizing the measurement dispersion must be developed. Forbes [8] employs a Bayesian approach to derive a posterior distribution for the form error boundary F from a finite sample drawn from a rectangular distribution with independent sampling or a Gaussian distribution with independent or correlated sampling, with the spatial correlation associated with the sampling modelled using Gaussian processes. This paper aims to extend the analysis to evaluate the associated risk and conformity assessment.

The paper is organised as follows. In Section 2, we discuss the form error model, which uses a uniform distribution with unknown boundaries to generate a posterior distribution using Bayesian inference. Using the provided posterior distribution, we generate expressions for conformance probability and specific risks associated with conformity assessment. In Section 3, we use the methods given in the previous sections to present a practical example. Section 4 then builds on the previous sections by considering a slightly more extended posterior model that takes into account the likely random effects of form errors as well as real form error data. Section 5 provides a second practical example of the extended posterior model for conformance evaluation. Finally, our concluding remarks are given in Section 6.

2. Model and methods

In this section, the form error estimates f_i for $i = 1, 2, \dots, m$ associated with points on the ideal surface are assumed to be drawn from a uniform distribution whose parameters are related to the form error boundary parameter $F > 0$ (more specifically, F is the boundary of the form error estimates as seen in Fig. 1). The aim is to use Bayesian inference to obtain a posterior distribution for F based on observed form error estimates f_i , and then to obtain explicit conformance and risk expressions.

2.1. The form error model based on a uniform distribution

Let the probability density function (PDF) of form error estimates f_i of a test item observed from a uniform distribution in the interval $[-F, F]$ after measuring $i = 1, 2, \dots, m$ points be given by:

$$g(f_i|F) \equiv U(f_i| -F, F) = (2F)^{-m},$$

otherwise $U(f_i| -F, F)$ is zero everywhere else. The symmetric nature of this distribution ensures that the mean, median and skewness are zero, and that the variance of this distribution is $F^2/3$. In practice, the observed form errors are subject to measurement uncertainty. We first consider the case where the measurement uncertainty is in much less than the true form error. Random effects associated with measurements are discussed in Section 4.

According to Bayesian inference, we can derive a posterior probability from two components: a prior probability and a likelihood function derived from a statistical model for the observed data. Since the form error data is given by $U(f_i| -F, F)$, then the likelihood function of associated with the model for the form error data is

$$\mathcal{L}(f|F) = \prod_{i=1}^m U(f_i| -F, F) \propto 1/F^m, \quad (1)$$

if $f_i \in (-F, F)$ and is zero otherwise. By regarding F as scale parameter, a suitable a non-informative prior PDF for F is $\pi_0(F) = 1/F$. Furthermore, if we let $F_0 = \max(|f_1|, \dots, |f_m|)$ such that $F \geq F_0$, then by Bayes' theorem, the combined posterior PDF results to a Pareto distribution:

$$\pi(F|m, F_0) = \frac{\mathcal{L}(f|F)\pi_0(F)}{\int_{F_0}^{\infty} \mathcal{L}(f|F)\pi_0(F)dF} = \frac{mF_0^m}{F^{m+1}}. \quad (2)$$

The parameter F_0 is the lower bound of the Pareto (which is the mode of the distribution). The Pareto is a skewed distribution with a decaying tail. As m increases, the tail decreases more quickly. Fig. 2 graphs (2) for various values of m for the case of $F_0 = 2 \mu\text{m}$. Table 1 shows that the posterior mean and median approaches F_0 as m increases.

2.2. Conformity and specific risk calculations

In conformity assessment, we wish to assign tolerance limits for a quantity to control the risks associated with making a wrong decision [9]. We shall use a Pareto posterior distribution in (2) to better understand the conformity method. We assume a production line manufactures circular parts that are measured, leading to form error estimates that are assumed to follow a Pareto distribution. To assess whether the form error complies with a specification, the measured value is compared to a tolerance interval. The conformance probability, denoted by p_c , is given by the set of conforming values for a one-sided tolerance interval from $[0, T]$, where T is the upper limit. For a Pareto distribution defined by m and F_0 ,

$$p_c = \int_{F_0}^T \pi(F|m, F_0)dF = 1 - (F_0/T)^m. \quad (3)$$

If the item does not conform with the specification, then the probability of non-conformance is $1 - p_c$. Note that the tolerance interval in (3) is actually $[F_0, T]$ instead of $[0, T]$. This is because the Pareto is defined for $F \geq F_0$.

JCGM 106 [9] published guidelines for such an assessment addressing two types of specific risks. Only binary decision criteria are evaluated, which means the item must either be deemed as accepted or rejected. As such, these risks can be obtained as a function of p_c . The first is the specific consumer's risk, denoted here as $R_c^S = 1 - p_c = (F_0/T)^m$, which is the probability that an accepted item will be non-conforming. The second is the specific producer's risk, $R_p^S = p_c = 1 - (F_0/T)^m$, which is the probability that a rejected item will be conforming. The calculation of conformance probabilities allows design of experiment questions to be answered, e.g., how many measurement points m are required to reduce risks to a specified level.

3. A practical example

In this section, we used a Pareto conformance function in (3) to

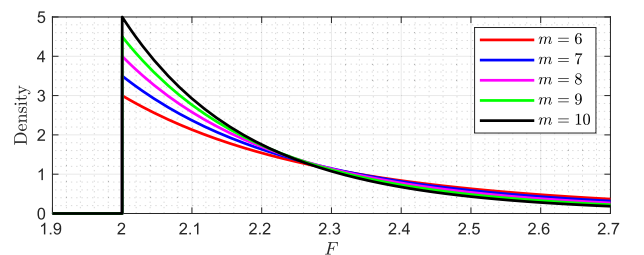


Fig. 2. Pareto distribution for various values of m starting with an observed value of $F_0 = 2 \mu\text{m}$.

Table 1

Pareto statistics for the posterior mean and median for the case of $F_0 = 2 \mu\text{m}$.

	Number of measured points (m)					
	5	10	20	50	100	200
Posterior mean (μm)	2.50	2.22	2.11	2.04	2.02	2.01
Posterior median (μm)	2.30	2.14	2.07	2.03	2.01	2.01

assess whether an item is accepted or rejected. We applied the conformance probabilities and risk formulas from the previous section to obtain varying conformance probabilities for different values of F_0 and m used (with a fixed T). For instance, if $F_0 = 2 \mu\text{m}$, $m = 10$ and $T = 3 \mu\text{m}$, then we accept an item with a conformance rate of 98.3% and an associated specific consumer’s risk of 1.7%. Table 2 summarizes the decisions made in response to various measurement results. Fig. 3 graphs the specific risks curves, respectively, for the case of $m = 10$.

4. Incorporating measurement uncertainty from random effects

A slightly more extensive posterior model, taking into consideration the probable random effects of form errors, is discussed here for the reader’s interest. The calculations in Section 2 assumed that the observed residual distances are accurate estimates of the surface’s form error estimates f_i for were free from some random effects. Suppose now that $d = f + \varepsilon$ where ε are random effects associated with a Gaussian distribution $N(0, \sigma_\varepsilon^2 I)$. In this case, we can use Bayesian inference to obtain a posterior distribution for the convolution of $f_i + \varepsilon_i$. The result of the sum of two independent continuous random variables has PDF:

$$g(z|F, m, \sigma_\varepsilon) = \int_{-F}^F U(|t| - F, F) N(z - t|0, \sigma_\varepsilon^2) dt,$$

by taking the likelihood of $g(z|F, m, \sigma_\varepsilon)$ after observing m measured points and setting a non-informative prior of $\pi_0(F) \propto 1/F$, the combined posterior PDF is therefore:

$$\pi(F|d, \sigma_\varepsilon) = \frac{C}{F^{m+1}} \prod_{i=1}^m \left[\text{erf}\left(\frac{F + d_i}{\sigma_\varepsilon \sqrt{2}}\right) + \text{erf}\left(\frac{F - d_i}{\sigma_\varepsilon \sqrt{2}}\right) \right]. \tag{4}$$

Here, the constant C is the assigned integrating factor to ensure that $\pi(F|d, \sigma_\varepsilon)$ integrates to one. This distribution reflects the measurement uncertainty affiliated with the residual distances examined, due to the randomness of σ_ε . Numerical integration is used to compute C , moments, quantiles and other common statistics associated with this PDF. The conformance probability and specific risks of (4) can be calculated numerically using the methods described in Section 2.2.

The posterior distribution of (4) is compared against the Pareto in Fig. 4 using real form error data after measuring 10 points around a circular item with a CMM. The following 10 form error measurements taken from the data points are 0.74, -0.46, -0.26, 0.14, -0.56, -1.86, 0.04, 0.04, 1.84 and 0.34 μm .

Here we compare the Pareto from (2) with the extended model from (4) using two values of σ_ε (differentiated by models A and B, which represents a σ_ε value equal to 1.0 and 0.4, respectively). For the

Table 2

Result of conformity assessment of a measured circular artefact under a Pareto posterior distribution from (2) for the case of $T = 3 \mu\text{m}$. *Item is accepted if $R_c^S \leq 5\%$.

Observed value (μm)	Measured points	Conformance probability	Specific consumer’s risk	Decision on the item*
2.0	10	98.3%	1.7%	Accept
2.0	15	99.8%	0.2%	Accept
2.3	10	93.0%	7.0%	Reject
2.3	15	98.1%	1.9%	Accept
2.6	10	76.1%	23.9%	Reject
2.6	15	88.3%	11.7%	Reject

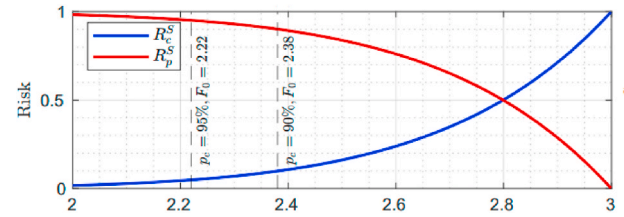


Fig. 3. Specific risk curves versus F_0 for making a wrong decision under a Pareto distribution for a tolerance limit of $T = 3 \mu\text{m}$. For conformity rates of 90% and 95%, the desired observed values are $F_0 = 2.38 \mu\text{m}$ and $F_0 = 2.22 \mu\text{m}$, respectively.

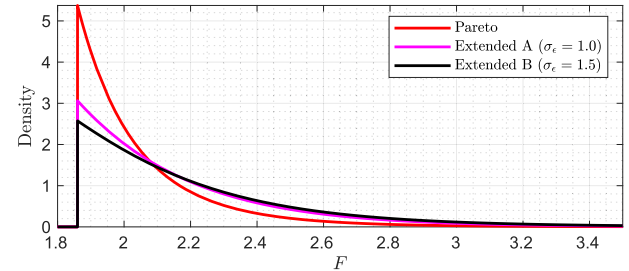


Fig. 4. Comparing the posterior PDFs of models (2) and (4). Real form error data was used for (4), with $F_0 = 1.86 \mu\text{m}$, $m = 10$ and different levels of σ_ε .

observed data, the minimum absolute form error is $F_0 = 1.86 \mu\text{m}$. Models A and B have mean values of 2.1889 and 2.2796 μm , respectively, which are higher than the Pareto mean of 2.0667 μm . Similarly, the standard deviations for both distributions are greater than the Pareto, at 0.3330 and 0.4160 μm , respectively, compared to 0.2311 μm . A basic distinction between the extended models and the Pareto is that the latter ignores measurement uncertainty. Although all distributions take little or no account of the probability values when $F < F_0$, the extended models takes the measurement uncertainty into consideration to provide a smoother, longer, and fatter tail. Thus increasing the value of σ_ε increases measurement uncertainty.

5. A second practical example

This section follows a similar procedure as Section 3. In this section, we are interested in using the extended model in (4) to calculate the conformance and specific risks. Table 3 illustrates the decisions made in response to real form error data utilizing a variety of inputs for σ_ε . For example, if $F_0 = 1.86 \mu\text{m}$ (calculated from real form error data), $m = 10$, $T = 3 \mu\text{m}$ and the random error is 0.25 μm , then we accept an item with a conformance rate of 98.53%, which is 0.63% less than the Pareto conformance rate (fixed at 99.16%). Fig. 5 graphs the specific consumer’s risk curves for different inputs of σ_ε .

In general, we find that increasing the random error reduces the conformance rate and increases the specific consumer risk, as expected. It also widens the difference between Pareto and extended model conformance rates. As a result, we find that measurement uncertainty has a significant impact on a measured item’s actual conformity rate.

6. Discussion and concluding remarks

This paper is concerned with developing a conformity assessment criterion for the form error model by comparing the distribution of its possible values to a tolerance interval using Bayesian inference, which takes measurement uncertainty and sampling effects into account. Most conformity assessment problems assume that the uncertainty associated with a quantity is Gaussian or Gaussian-like. For form error assessment, the associated distribution is far from a Gaussian. Through Bayesian

Table 3

Result of conformity assessment of a measured circular artefact under the extended model from (4) for the case of $T = 3 \mu\text{m}$ and $m = 10$. *Item is accepted if $R_c^s \leq 5\%$.

Observed value (μm)	Random error (μm)	Conformance probability	Difference from Pareto using (3)	Specific consumer's risk	Decision on the item
1.86	0.25	98.53%	0.63%	1.47%	Accept
1.86	0.50	98.07%	1.09%	1.93%	Accept
1.86	1.00	96.90%	2.27%	3.10%	Accept
1.86	1.50	93.65%	5.51%	6.35%	Reject

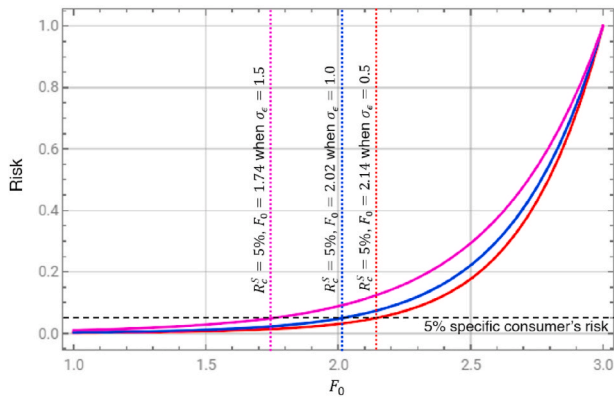


Fig. 5. Specific consumer's risk curves versus F_0 for making a wrong decision under model (4) for a tolerance limit of $T = 3 \mu\text{m}$. For a risk of less than 5%, the desired observed values are $F_0 = 2.14 \mu\text{m}$, $2.02 \mu\text{m}$ and $1.74 \mu\text{m}$ when $\sigma_e = 0.5 \mu\text{m}$, $1.0 \mu\text{m}$ and $1.5 \mu\text{m}$, respectively.

inference, we derived a posterior PDF (Pareto) by considering the likelihood of measurement data (e.g., a uniform distribution with unknown form error bounds) and a prior distribution, to describe the form error model.

The posterior model was then extended by integrating measurement uncertainty from the likely random effects of form errors, which was addressed in Section 4 and followed by some interesting results in Section 5 for the reader's interest. The approaches discussed in this paper disregard the fact that form error estimates at the surface points are determined due to surface fitting, and therefore they are subject to a correlating effect associated with the fitting.

The definite integral of the posterior PDF for a given range is the most significant step in the conformance and specific risk calculations, and so these calculations are straightforward for univariate distributions when using their cumulative distribution function.

Acknowledgments

The first author would like to thank the sponsorship of Brunel University London for his PhD studies.

References

- [1] A.B. Forbes, Least Squares Best Fit Geometric Elements, *Algorithms for Approximation II*, 1990, pp. 311–319.
- [2] A.B. Forbes, H.D. Minh, Form assessment in coordinate metrology, *Approximation Algorithms for Complex Systems 3* (Dec. 2010) 69–90.
- [3] G.A. Watson, *Approximation Theory and Numerical Methods*, 1997. New York.
- [4] N.N. Abdelmalek, On the discrete linear l1 approximation and l1 solutions of overdetermined linear equations, *J. Approx. Theor.* 11 (1) (1974) 38–53.
- [5] G.A. Watson, A method for the Chebyshev solution of an overdetermined system of complex linear equations, *IMA J. Numer. Anal.* 8 (4) (1988) 461–471.
- [6] K. Madsen, An algorithm for minimax solution of overdetermined systems of non-linear equations, *IMA J. Appl. Math.* 16 (3) (1975) 321–328.
- [7] M.R. Osborne, G.A. Watson, An algorithm for minimax approximation in the nonlinear case, *Comput. J.* 12 (1) (1969) 63–68.
- [8] A.B. Forbes, Uncertainty associated with form assessment in coordinate metrology, *Int. J. Metrol. Qual. Eng.* 4 (1) (2013) 17–22.
- [9] BIPM, IEC, IFCC, ILAC, ISO, IUPAC, IUPAP, OIML, Evaluation of measurement data — the role of measurement uncertainty in conformity assessment [Online]. Available: https://www.bipm.org/utls/common/documents/jcgm/JCGM_106_2012_E.pdf, 2012.

Yacine Koucha*

Brunel University London, Uxbridge, UK

Alistair Forbes

National Physical Laboratory, Teddington, UK

E-mail address: Alistair.Forbes@npl.co.uk.

QingPing Yang

Brunel University London, Uxbridge, UK

E-mail address: QingPing.Yang@brunel.ac.uk.

* Corresponding author.

E-mail address: Yacine.Koucha@brunel.ac.uk (Y. Koucha).